Analysis of Sugar Bioprotective Mechanisms on the Thermal Denaturation of Lysozyme from Raman Scattering and Differential Scanning Calorimetry Investigations

A. Hédoux,*,† J-F. Willart,† R. Ionov,‡ F. Affouard,† Y. Guinet,† L. Paccou,† A. Lerbret,† and M. Descamps†

Laboratoire de Dynamique et Structure des Matériaux Moléculaires, UMR CNRS 8024, Université de Lille 1, UFR de Physique, Bat. P5, 59 655 Villeneuve d'Ascq Cedex, France, and College of Sciences "Leonardo da Vinci", P.O. Box 946, BG 1000 Sofia, Bulgaria

Received: March 14, 2006; In Final Form: July 24, 2006

Sugar-induced thermostabilization of lysozyme was analyzed by Raman scattering and modulated differential scanning calorimetry investigations, for three disaccharides (maltose, sucrose, and trehalose) characterized by the same chemical formula ($C_{12}H_{22}O_{11}$). This study shows that trehalose is the most effective in stabilizing the folded secondary structure of the protein. The influence of sugars on the mechanism of thermal denaturation was carefully investigated by Raman scattering experiments carried out both in the low-frequency range and in the amide I band region. It was determined that the thermal stability of the hydrogen-bond network of water, highly dependent on the presence of sugars, contributes to the stabilization of the native tertiary structure and inhibits the first stage of denaturation, that is, the transformation of the tertiary structure into a highly flexible state with intact secondary structure. It was found that trehalose exhibits exceptional capabilities to distort the tetra-bonded hydrogen-bond network of water and to strengthen intermolecular O−H interactions responsible for the stability of the tertiary structure. Trehalose was also observed to be the best stabilizer of the folded secondary structure, in the transient tertiary structure, leading to a high-temperature shift of the unfolding process (the second stage of denaturation). This was interpreted from the consideration that the transient tertiary structure is less flexible and inhibits the solvent accessibility around the hydrophobic groups of lysozyme.

Introduction

Proteins are the principal units that govern the functions of living systems. Under extreme conditions (temperature, high pressure, desiccation), proteins may denature. Many organisms have evolved efficient techniques to protect proteins, one example is sugar synthesis. Moreover, sugars are used in freeze-drying procedures of therapeutic proteins to preserve their activity.[1] Among several sugars, trehalose is recognized to be very effective in the stabilization of macromolecules against thermal inactivation,[2] of therapeutic proteins (characterized by short shelf lives) during freeze-drying,[3] and exposure to high temperatures in solutions.[4] In recent years, extended physiological and biological studied have shown that the disaccharide trehalose is particularly found in high concentrations in many living organisms which have the ability to survive severe external stresses. Several hypotheses have been suggested to explain the superior effectiveness of trehalose. Some of them involve direct biomolecule−sugar−water interactions[4,5] or specific properties of sugar−water solutions concerning the vitrification of the solutions[6] or the influence of sugars on the water tetrahedral hydrogen-bond network.[7] Extended investigations of water−sugar solutions have revealed specific signatures of trehalose with respect to other sugars both on the physical properties (temperature dependence of molecular mobility) of the solutions[6,8−10] and on the structure of the water hydrogen-bond network.[11−14]

This paper focuses on the protective action of additive sugars in lysozyme−water solution during the process of thermal denaturation to determine the mechanism of bioprotection by sugars on thermal denaturation and to determine the specific properties of trehalose which make it a better bioprotector than other disaccharides.

The biological activity of proteins depends on their three-dimensional structure, which is closely connected to hydration. It is generally believed that the conformational stability of most proteins results from a combination of conflicting effects: hydrophobicity and hydrogen bonding. The addition of stabilizing solutes to aqueous solutions has a direct influence on the nature of both conflicting interactions between proteins and solvent, and thus on the structure and the stability of the native state of proteins.

A recent investigation[15] by Raman spectroscopy and modulated differential scanning calorimetry (MDSC) on lysozyme dissolved in H_2O and D_2O has shown that the thermal denaturation process can be described in two stages. The first stage corresponds to a change in the tertiary structure without concomitant unfolding of the secondary structure. An important consequence of this change is an increased solvent penetration which is probably responsible for the destabilization of the molecular conformation through the breaking of the subtle balance between hydrophobic and hydrophilic interactions. The transformation from native-to-transient tertiary structure, characterized by increased hydrophobic interactions in the protein interior, appears to be a precursor to the second stage of thermal denaturation, that is, the unfolding process of the secondary structure. Such an intermediate state was previously reported

* To whom correspondence should be addressed. E-mail: alain.hedoux@univ-lille1.fr.

† Université de Lille 1.

‡ College of Sciences "Leonardo da Vinci".

10.1021/jp061568i CCC: $33.50
Published on Web 10/17/2006

by different kinds of investigations[16−19] and can be associated with the so-called molten globule state.[17,20−24] The study of lysozyme dissolved in H_2O and D_2O has revealed the crucial influence of the hydrogen-bond (H-bond) network of water on the stability of the tertiary structure.

In this paper, we report an analysis of the influence of three disaccharides (maltose, sucrose, and trehalose) during these two stages of denaturation to determine their role in the protection mechanism of the biological activity of lysozyme against thermal denaturation. The capability of the three sugars to form H-bonds with protein or water is directly comparable since these homologous disaccharides have the same chemical formula, $C_{12}H_{22}O_{11}$, and the same number of hydroxyl groups. The ternary mixtures (water/sugar/lysozyme) are analyzed by Raman spectroscopy and MDSC during heating from 298 to 373 K. Raman spectroscopy in the low-frequency range of 10−350 cm^{-1} and in the high-frequency range of the amide I band region, 1500−1800 cm^{-1}, allows us to analyze separately the two stages of thermal denaturation, while MDSC provides us with information on the temperature and enthalpy of the overall transformation.

These results are compared with those obtained from the analysis of the lysozyme−water solutions,[15] without the sugars. To obtain a better insight into the influence of trehalose on the different stages of thermal denaturation, trehalose was mixed in D_2O prior to addition of lysozyme. In light of previous studies which have shown that D_2O can be used as a marker of solvent penetration[15,25−27] in the protein interior allows us to analyze the transformation that involves the transient tertiary structure.

Material and Methods

Lysozyme from chicken egg white (14.3 kDa) is supplied from Sigma. High-purity maltose monohydrate, sucrose, and trehalose dihydrate were supplied from Fluka and Sigma. First, the sugar−water mixtures were prepared at the appropriate concentration, and thereafter, the protein was added. Ternary solutions with 40% mass sugar concentration were systematically analyzed by Raman scattering and MDSC, and solutions with 10, 20% mass trehalose concentrations were only analyzed by MDSC. The protein-containing mixtures were agitated in an Eppendorf agitator at about 298 K with about 1000 turns/min. Sugar/water weight proportions were prepared using double-distilled pure water. A lysozyme concentration of about 14.58×10^{-3} mol/L was used to ensure about 10 water hydration shells surrounding the protein molecules in water that limits the direct protein−protein interactions. Measurements were carried out in the 295−380 K temperature range on samples at pH 6.5.

MDSC Experiments. The MDSC experiments were performed using the MDSC 2920 microcalorimeter of TA instruments. The temperature and enthalpy readings were calibrated using pure indium. Only heating runs were performed with a scanning rate of 2 K/min. To analyze the thermodynamic features of the polyamorphic transition, suitable modulation parameters are found to be 40 s for the period of modulation and a modulation amplitude of 0.212 °C. The C_p reading was calibrated using a standard sapphire sample in the temperature range of study.

The enthalpy of denaturation, ΔH, was determined by integration of the C_p trace using the sigmoidal tangents above and below the denaturation peak as a baseline. The C_p jump detected from the difference in the baseline on both sides of the endothermic peak was then systematically determined for each sample. This jump can be associated with the peak observed on the trace corresponding to the phase lag of the modulated heat flow with respect to the modulated temperature, usually characteristic of a glasslike transition.[28,29]

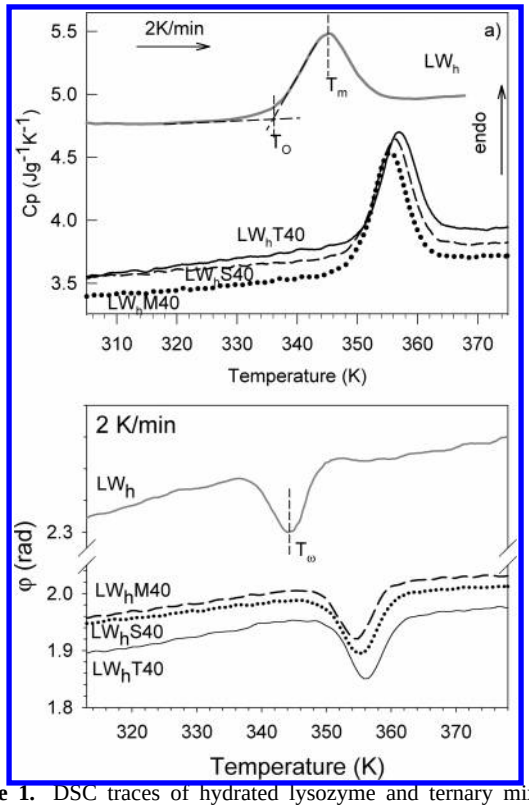

Figure 1. DSC traces of hydrated lysozyme and ternary mixtures (LWhM40, LWhS40, and LWT40): (a) Cp signal and (b) phase lag φ between the heat oscillations and the temperature oscillations.

Raman Spectra. Raman spectra were recorded in the 10−300 cm^{-1} range and in the 1500−1800 cm^{-1} range by measuring in backscattering geometry and using a XY Dilor spectrometer with a 514.5 nm Ar−Kr laser and 20 mW of incident power. The mixtures were loaded in Hellma quartz-suprasil cells and hermetically sealed. A weak fluorescence contribution to the spectra appeared systematically in the background signal. Its magnitude was approximated by a second-order polynomial using a fitting procedure and then subtracted from the spectra. In a previous study,[15] a possible H ↔ D exchange with time at 298 K was analyzed by using the Raman spectra of the LW_d mixture obtained in the above given two spectral ranges over a period of 72 h. No significant modification of the spectra was observed during this period at 298 K, indicating that the H ↔ D exchange was insignificant if any at all.

Results

MDSC Measurements. The C_p and phase angle φ measured upon heating lysozyme + H_2O (LW_h) and lysozyme + H_2O + sugar (LW_hM40, LW_hS40, and LW_hT40 for 40% maltose, sucrose, and trehalose dissolved in water) are reported in Figure 1. In Figure 1a, an endothermic peak is systematically observed for each sample. The endotherms yield the onset temperature, T_O^{DSC}, the melting temperature, T_m^{DSC}, as labeled in Figure 1a, and the calorimetric enthalpy ΔH. These values are listed in Table 1. The jump in the C_p value, ΔC_p, which is clearly observed for each sample, was previously associated with the peak of phase lag (φ),[15] shown in Figure 1b. The ΔC_p value and the temperature of the peak phase, T_ω, are also reported in Table 1. The data in Table 1 and Figure 1 show that both T_ω

TABLE 1: Thermodynamical Parameters of the Thermal Denaturation Obtained from MDSC Measurements on LWh, L(W_h + w%Sugar), and L(W_d + w%T) Samples

samples	T_ω (K)[a]	T_O^{DSC} (K)[b]	T_m^{DSC} (K)[b]	ΔH (J/g)[b]	ΔC_p (J/g·deg)
LW_h	344.1 ± 0.1	340.4 ± 0.1	346.3 ± 0.1	5.4 ± 0.3	0.06 ± 0.01
LW_hM40	354.5 ± 0.1	350.1 ± 0.1	355.2 ± 0.1	5.6 ± 0.3	0.06 ± 0.01
LW_hS40	355.2 ± 0.1	350.4 ± 0.1	355.9 ± 0.1	6.5 ± 0.3	0.05 ± 0.01
LW_hT40	356.2 ± 0.1	351.9 ± 0.1	356.7 ± 0.1	6.3 ± 0.3	0.05 ± 0.01
LW_d	346.0 ± 0.1	343.4 ± 0.1	348.6 ± 0.1	4.8 ± 0.3	0.05 ± 0.01
LW_dT20	351.5 ± 0.1	346.9 ± 0.1	352.4 ± 0.1	4.9 ± 0.3	0.06 ± 0.01
LW_dT40	358.2 ± 0.1	353.4 ± 0.1	358.8 ± 0.1	5.6 ± 0.3	0.05 ± 0.01

[a] T_ω is the temperature of the phase peak plotted in Figure 1b. [b] T_O^{DSC}, T_m^{DSC}, and ΔH are determined from the endothermic peaks shown in Figure 1A.

and T_m^{DSC} shift to high temperatures with the addition of the sugars. Table 1 also reveals that ΔH is higher for the ternary mixtures, especially for LW_hT40 and LW_hS40 samples. As expected, the addition of trehalose induces a significantly larger shift in T_ω and T_m^{DSC} than the addition of sucrose or maltose. Maltose appears to be the least efficient among the three sugars in preventing thermal denaturation of hydrated lysozyme. The temperature of the phase peak T_ω was considered as the signature of the first stage of thermal denaturation, that is, the transformation of the native tertiary structure into a more flexible structure without concomitant unfolding of the secondary structure.[15] Consequently, Table 1 shows that the addition of sugars increases T_ω, that is, sugars stabilize the native tertiary structure. It is also observed that the addition of sugars has no significant influence on ΔC_p which has been associated with the first stage of denaturation. It is worth noting that the ΔC_p values for the LW_h and LW_d samples listed in Table 1 are very weak and the addition of 40% sugar in hydrated lysozyme with high water content could have a weak influence on the amplitude of the C_p jump, not detectable with the experimental device used in this study. It was previously observed that lysozyme dissolved in D_2O denatures at a higher temperature than that dissolved in H_2O. A shift of denaturation toward higher temperatures is also observed between LW_hT40 and LW_dT40 samples.

Raman Scattering Investigations: Scattered Low-Frequency Intensity. The scattered low-frequency intensity is composed of quasielastic intensity and harmonic vibrations which overlap in the 10−100 cm^{-1} range. It was transformed into reduced intensity, defined by $I_r(\nu) = I(\nu)/(\nu[n(\nu) + 1])$, where $n(\nu)$ is the Bose factor. This transformation enhances the observation of the quasielastic contribution. The two contributions to the Raman intensity were estimated by using a fitting procedure of the reduced intensity with a Lorentzian line-shape for the first contribution (quasielastic) and a log−normal distribution function for the second (harmonic vibrations).[15,30] After the quasielastic contribution was subtracted from the spectra, the Raman intensity was transformed into Raman susceptibility ($\chi''(\nu) = \nu I_r(\nu)$). This contribution is related to $g(\nu)$ the vibrational density of state (VDOS), by $\chi''(\nu) = (C(\nu)\text{-}g(\nu)/\nu)$, where $C(\nu)$ is the light-vibration coupling coefficient. It is usually observed that $C(\nu)$ has a linear ν-dependence in the Boson peak (BP) region,[31−33] and the Raman susceptibility is then considered as representative of the VDOS ($\chi''(\nu) \propto g(\nu)$). The Raman susceptibility $\chi''(\nu)$ of the hydrated lysozyme (LW_h) is plotted in the native (Figure 2a) and denatured states (Figure 2b), and $\chi''(\nu)$ of the three ternary mixtures (LW_hM40, LW_hS40, and LW_hS40) is plotted in parts c and d of Figure 2. The plot of $\chi''(\nu)/\nu^2$ is generally used to determine the excess of VDOS corresponding to BP if $\chi''(\nu) \propto g(\nu)$ is used in the analysis. This plot is shown in Figure 3 for the hydrated lysozyme and the three ternary mixtures in the native and denatured states. Only the excess of VDOS (BP) of lysozyme + D_2O + 20%, 40%trehalose mixture (LW_dT40) are plotted in Figure 4 with the BP of the LW_d sample in both the native and

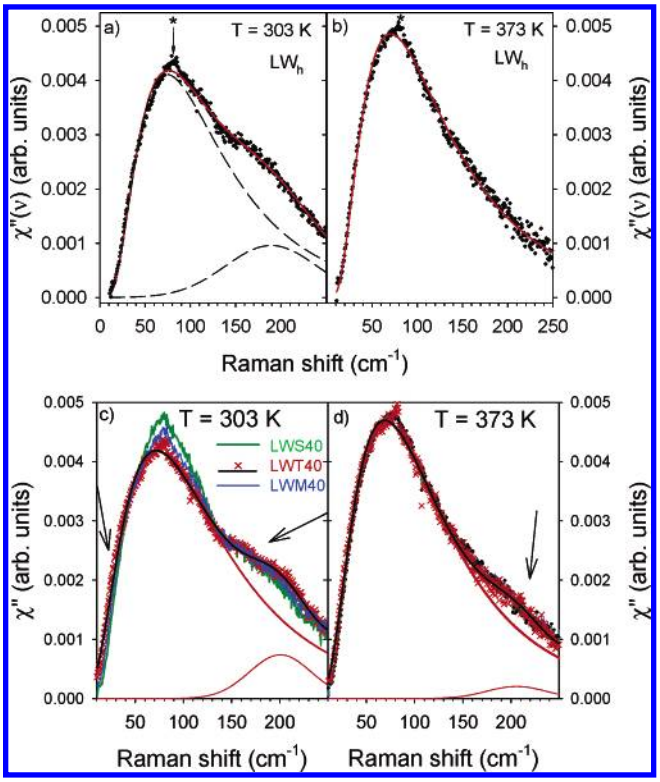

Figure 2. Experimental Raman susceptibility and fitting procedure in hydrated lysozyme in the native and denatured states, respectively, (a) and (b). In the native state, $\chi''(\nu)$ is fitted using two bands (dashed lines) corresponding to a log−normal distribution assigned to the protein dynamics and solvent−protein interaction and a Gaussian line shape assigned to the intermolecular O−H stretching vibrations in the H-bond network of water. In the denatured state, only one band (log−normal distribution) is needed to fit experimental data and thus corresponds to the fit of $\chi''(\nu)$. The fit of susceptibility corresponds to the red line. The stars localize laser excitation. Experimental Raman susceptibility in LW_hT40 (red X), LW_hM40 (blue line), and LW_hS40 (green line) mixtures in the native and denatured states, respectively, is shown in parts (c) and (d). Only the bands resulting from the fitting procedure in LW_hT40 are plotted as red lines, and the fit of $\chi''(\nu)$ is plotted in the black line. A residual intensity can be observed corresponding to the intermolecular O−H stretching vibrations in water.

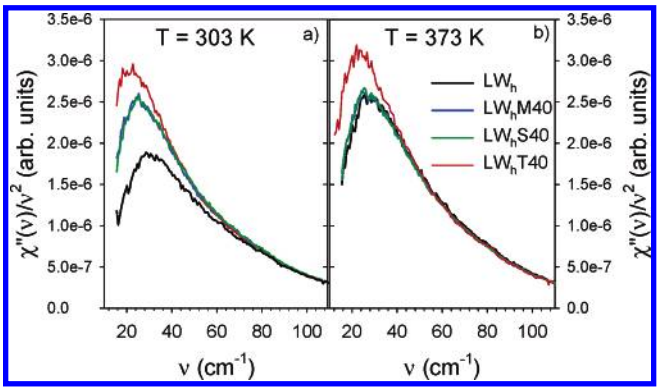

Figure 3. A ($\chi''(\nu)/\nu^2$) plot representative of the excess of VDOS and considered as the boson peak (BP) representation in (a) the native state and (b) in the denatured state. In the native state, the addition of sugar induces an increase of the excess of VDOS more pronounced for trehalose. In the denatured state, only the LW_h sample exhibits a significant enhancement of VDOS excess.

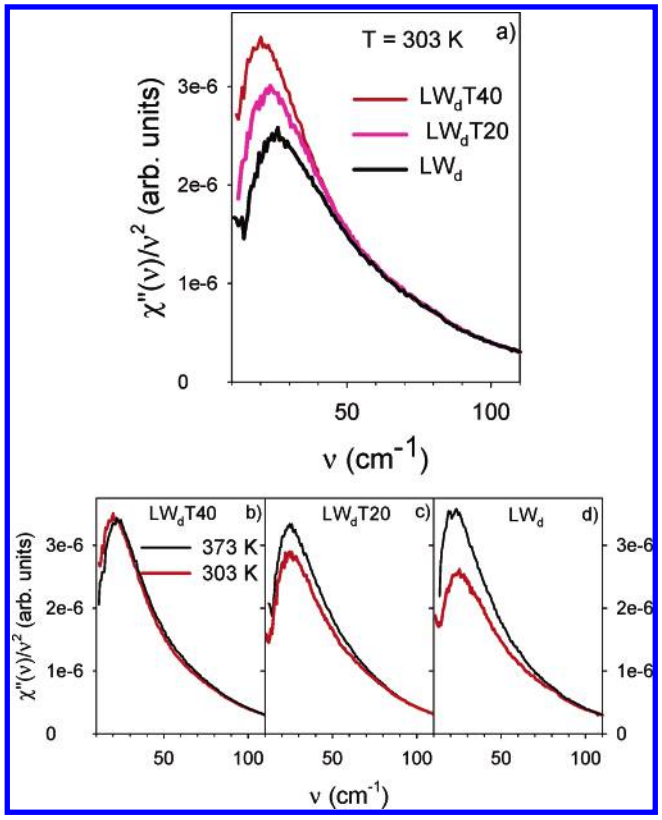

Figure 4. Comparison of ($\chi''(\nu)/\nu^2$) plots (BP) in LW_d, LW_dT20, and LW_dT40 mixtures: (a) comparison of the three mixtures in the native state, and comparison between the native and denatured states (b) for LW_dT40, (c) Lw_dT20, and (d) LW_d. The VDOS excess increases with trehalose content in the native state, and thermal denaturation induces a significant enhancement of the VDOS excess for low sugar content.

denatured states. As reported in the previous study of hydrated lysozyme,[15] in the native state $\chi''(\nu)$ is composed of two broad Raman bands (Figure 2a) and can be fitted using a log−normal distribution (for the lowest-frequency band) and Gaussian lineshape (for the highest-frequency band) corresponding to

$$\chi_{fit}(\nu) = H(\nu_1)\exp\left[-\frac{1}{2}\left(\frac{\ln\frac{\nu}{\nu_1}}{W_1}\right)^2\right] + H(\nu_2)\exp\left[-\frac{1}{2}\left(\frac{\nu-\nu_2}{W_2}\right)^2\right] \quad (1)$$

where ν_1 and ν_2 are the frequencies at the peak maxima $H(\nu_1)$ and $H(\nu_2)$, respectively, and W is the line width. In the denatured state of the hydrated lysozyme, the Raman susceptibility can be satisfactorily fitted using only the log−normal distribution, as is shown in Figure 2b.

Influence of Sugars on the Low-Frequency Raman Spectrum of Hydrated Lysozyme in the Native and Denatured States. *Native State.* In the native state at $T = 303$ K, each spectrum shown in Figure 2c is also composed of two broad bands. The high-frequency band which is more prominent at ~180 cm^{-1} in hydrated lysozyme (LW_h) was previously assigned[15] to collective O−H stretching vibrations in the hydrogen-bond network of water. The low-frequency band mainly corresponds to harmonic vibrations in lysozyme but also reflects the dynamics of the solvent−proteins interface which has been considered to be responsible for the appearance of BP.[15,34,35] The addition of sugar in the hydrated lysozyme induces two main changes in the Raman susceptibility indicated by arrows in Figure 2c. The first arrow shows an enhancement of the VDOS in the very low-frequency range which can be easily observed in the plot of BP in Figure 3a. This change indicates increased solvent−lysozyme interactions in the solvent−protein interface, probably via H-bonds in ternary mixtures with regard to the hydrated lysozyme. Figure 3a also clearly reveals that addition of trehalose induces the strongest enhancement of the VDOS, that is, the strongest enhancement of solvent−lysozyme interactions. From these experiments, it is not possible to discriminate between additional water−lysozyme and sugar−lysozyme interactions as being responsible for the enhancement of the VDOS. The second arrow in Figure 2c shows the decrease of the susceptibility of the broad band corresponding to O−H stretching vibrations in the H-bond network of water with the addition of sugar, indicative of the distortion of the tetrahedral H-bond network of water.

The Raman susceptibility in the LW_dT40 mixture exhibits similar features with regard to the LW_d sample, that is, an enhancement of the VDOS in the low-frequency range, which is clearly observed in the $\chi''(\nu)/\nu^2$ plot in Figure 4a and a decrease of the intensity of the intermolecular O−D stretching band.

Denatured State. In the denatured state at 373 K, the line shape of Raman susceptibilities of hydrated lysozyme and ternary mixtures plotted in Figure 2d are very similar. However, the addition of sugar can be characterized by the observation of a residual susceptibility around 200 cm^{-1} (localized by the arrow in Figure 2d) which is not observed in the spectrum of hydrated lysozyme in the denatured state (Figure 2b). During the heating of hydrated lysozyme, the downshift and the disappearance of the 180 cm^{-1} band have been observed earlier[15] and interpreted as reflecting the breaking of hydrogen bonds in the H-bond network of water. Consequently, the addition of sugars seems to stabilize the distorted H-bond network of water. A more detailed investigation of the Raman susceptibility in the very low-frequency range can be performed from the plot of BP in Figure 3b. It is observed that the BP of the LW_hM40 and LW_hS40 mixtures is superimposed on the BP of hydrated lysozyme, while an enhancement of the excess of VDOS in the LW_hT40 mixture with regard to other ternary mixtures, already existing in the native state, is clearly detected. The increase of the intensity of the BP in hydrated lysozyme has been previously observed to accompany the enhanced water accessibility in the protein interior.[15] Consequently, Figure 3 shows that the enhancement of the VDOS between the native and denatured states is reduced by the addition of sugar. This is interpreted as a limitation of the solvent penetration in the transient tertiary structure. Above the transformation of the native tertiary structure ($T > T_\omega$) no change of the low-frequency Raman spectra is observed, indicating that the unfolding process has no significant influence on the protein and solvent−protein interface dynamics. The difference between LW_hT40 and other samples can be assigned to more increased interactions between water−trehalose and lysozyme than between maltose or sucrose and lysozyme both in the native and in the denatured states.

The BP in the denatured state of LW_dT40 (Figure 4b) is very similar to that in the native state. It can be interpreted as the limitation of the solvent accessibility in the protein interior probably induced by a similar flexibility of the tertiary structure in both native and denatured states.

Raman Spectrum in the Amide I Band Region. The Raman spectrum of hydrated lysozyme and of the three ternary mixtures (LW_hM40, LW_hS40, and LW_hT40) in the 1500−1765 cm^{-1} spectral range are shown at 303 K in Figure 5a. This region is

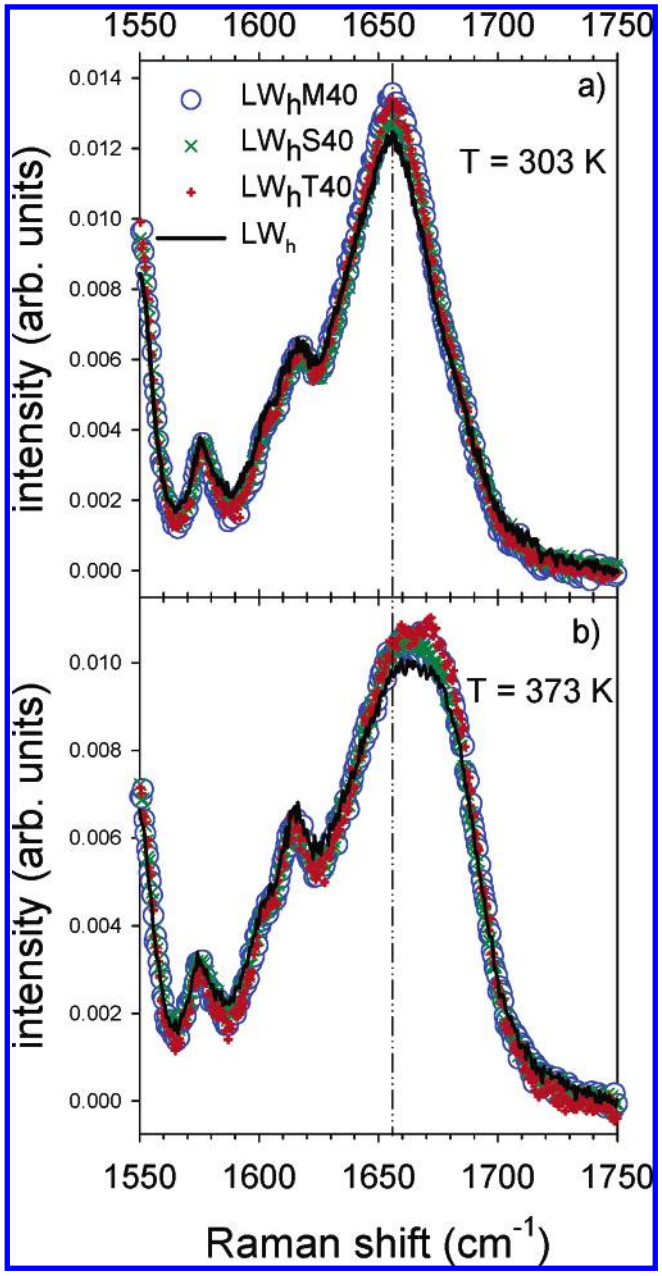

Figure 5. Raman spectra in the amide I band region (1550−1750 cm^{-1}) of LW_h, LW_hM40, LW_hS40, and LW_hT40 samples (a) in the native state and (b) in the denatured state. Raman spectra of the lyso/water sample are superimposed with spectra of lyso/water/sugars samples both in the native and in the denatured states.

dominated by a broad Raman band near 1657 cm^{-1} corresponding to the C═O stretching vibration (amide I band) of amide groups coupled to the in-phase bending of the N−H bond and the stretching of the C−N bond.[26] The extreme similarity between the Raman spectra of the amide I band confirms that the previous studies[36,37] are indicative of a similar secondary structure in a sugar or water environment.

The Raman spectrum of the same samples in their denatured state is plotted in Figure 5b. The superposition of the spectra shows that denatured lysozyme has the same molecular conformation in water or sugar environment and that addition of sugars has no influence on the unfolding secondary structure.

The analysis of this band during heating allows us to monitor the transformation of the molecular conformation, that is, the unfolding of the α-helix secondary structure. The Raman band observed near 1610 cm^{-1} was assigned to the intermolecular

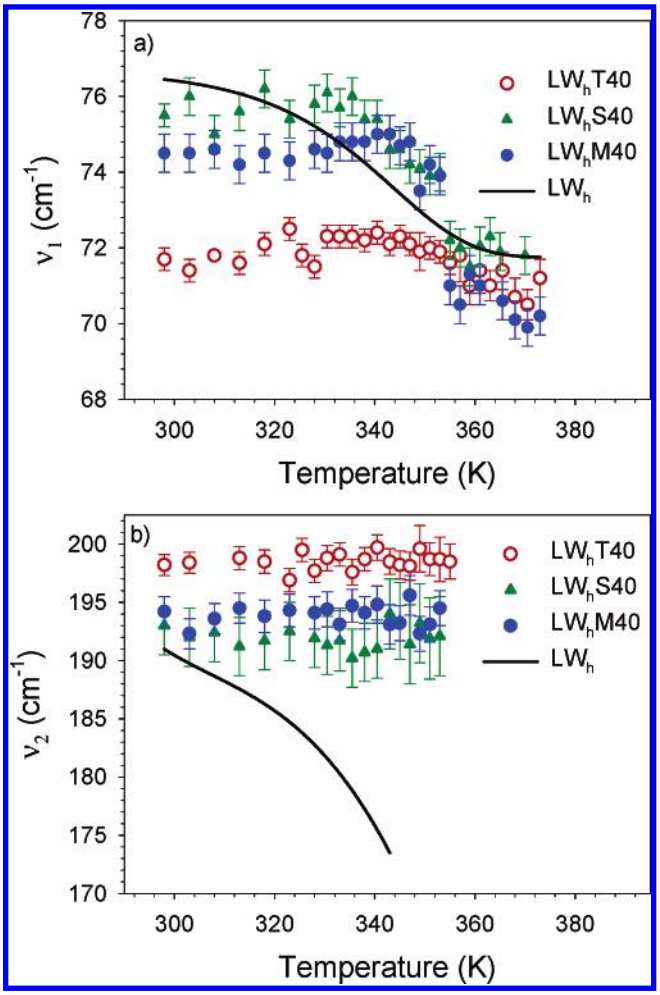

Figure 6. Temperature dependence of the frequency (ν_1) of the lowest-frequency band (a) and the frequency (ν_2) of the intermolecular O−H stretching band in the H-bond network of water in LW_hM40, LW_hS40, and LW_hT40 samples compared with the LW_h sample. The two temperature dependences in the LW_h sample are plotted in a black line for better clarity.

β-sheet interactions and can be used as a probe to detect molecular aggregation via the increase of its intensity.[25,27] An inspection of Figure 5 shows that no molecular aggregation is detected in the LWM40, LWS40, and LWT40 samples, as was previously observed for the hydrated lysozyme.[15]

Analysis of Raman Spectra. The Raman susceptibility of ternary mixtures reported in Figure 2 is analyzed by a fitting procedure (1).

The temperature dependence of the frequency of these two bands is reported in Figure 6 for each sample. It is compared with that previously determined in the hydrated lysozyme[15] plotted as a continuous line for clarity. As for hydrated lysozyme, special features are observed for the temperature dependence of both bands at temperatures (T_ω) corresponding to the phase signal peaks detected in the MDSC experiments (Figure 1b). These features correspond to the change in the line shape of the low-frequency Raman susceptibility which occurs during the transformation into the transient tertiary structure. However, addition of sugar gives rise to drastic changes on the temperature dependence of the two Raman bands detected below 250 cm^{-1}.

First, the lowest-frequency band is observed at lower frequencies and exhibits a downshift at higher temperatures in ternary mixtures than in the LW_h sample (Figure 6a). This downshift is observed at a temperature corresponding to T_ω reported in

Table 1. The lowering of the ν_1 frequency in the native state by addition of sugar is related to the excess of VDOS observed through the plot of $\chi''(\nu)/\nu^2$ (Figure 3a). Figure 6a points out a special behavior of the mixture with trehalose according to the plot of the BP (Figure 3).

Second, the high-frequency band observed around 190 cm^{-1} in the hydrated lysozyme exhibits temperature independence in ternary mixtures contrasting with the temperature dependence determined in LW_h (continuous line in Figure 6b). However, the intensity of this band decreases with an increase in temperature and practically disappears around T_ω, as observed in Figure 2b. The ν_2 frequency cannot be significantly determined by the fitting procedure, although some spectral tail in the high-frequency side of the lowest-frequency band remains observable (Figure 2b). Figure 6b reveals that ν_2 increases by addition of sugar and thus hydrogen-bonding interactions increase in the network structure of water. It is also very noticeable that the highest ν_2 value is obtained in the trehalose mixture. Moreover, the residual contribution of this band above T_ω is most important in the presence of trehalose.

The temperature dependence of the amide band frequency is fitted by the equation, $\nu = [(\nu_N - \nu_D)/(1 + \exp((T - T_m)/\Delta T))] + \nu_D$, where T_m is the transition midpoint temperature, $2 \times \Delta T$ corresponds to the temperature domain of the transition, and ν_N and ν_D are the frequencies of the amide band in the native and denatured states, respectively. For comparison, a least-squares fit of experimental data is plotted in Figure 8a for the ternary mixtures and for hydrated lysozyme LW_h taken from a recent paper.[15] The onset temperature, T_O can also be determined for the helical unfolding, as shown in Figure 7a. T_O, T_m (noted T_O^{Ram} and T_m^{Ram} in Table 2), and ΔT are listed in Table 2. It is clearly observed that the addition of sugars leads to a shift of the unfolding curve toward higher temperatures. It is also noted that the unfolding process is systematically observed at a temperature slightly higher than T_ω corresponding to the peak of φ (see Table 1). However, the shift of the temperature, T_m^{Ram}, as determined by least-squares refinements reported in Table 2, results from both the shift of T_ω and the increase of ΔT. Both are more pronounced for the LW_hT40 sample.

The denaturation curve can be analyzed on the basis of a two-state native (N)−denatured (D) reversible transition.[38,39] The free energy change ΔG_{ND} which controls the transition is determined from $\Delta G_{ND} = -RT \ln K$, where R is the gas constant, T the temperature, and $K = p_D/p_N = (\nu_N - \nu)/(\nu - \nu_D)$, the equilibrium ratio of the population probabilities p_D and p_N. From the fit of experimental data, the net sugar stabilization free energy $\Delta(\Delta G_{ND}) = \Delta G_{ND}$ (sugar) $- \Delta G_{ND}$ (water) was determined for the unfolding process. These values, reported in Table 2, confirm that all three sugars stabilize and shift the unfolding process toward higher temperatures and trehalose is the most effective stabilizer of the secondary structure.

The temperature dependence of the frequency of the amide I band is reported in Figure 8b for the LW_dT40 and LW_dT20 ternary mixtures, and lysosyme + D_2O (LW_d) taken from a recent study.[15] The frequency of the amide I band in the folding state is nearly the same in the three samples. It is lowered with regard to that in mixtures with H_2O, because of NH/ND exchange. Figure 7b reveals a downshift of the amide band frequency, previously assigned to an enhanced solvent accessibility, which is observed to be dependent on the sugar content. This observation is in agreement with very weak changes detected in the low-frequency Raman line shape between the native and denatured states, corresponding to an increase in VDOS excess (parts b, c, and d of Figure 4), also assigned to the solvent penetration in the protein interior.

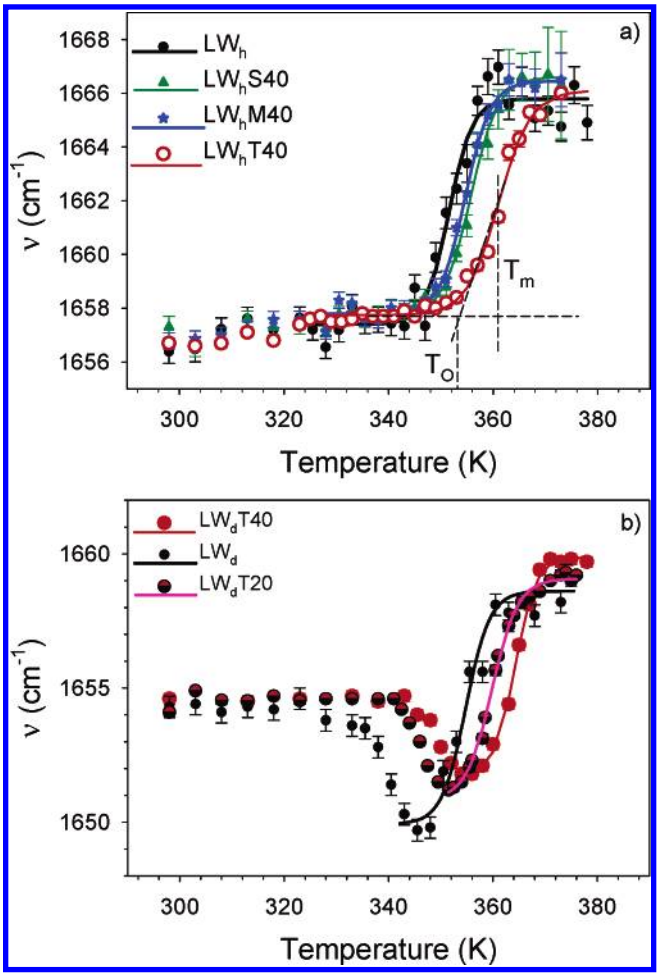

Figure 7. Temperature dependence of the amide I band frequency (a) in lysozyme mixed with H_2O and w40% sugars and (b) in lysozyme mixed with D_2O and w20%, w40% trehalose. T_m and T_o are represented for the LW_hT40 sample. The lines correspond to the fitting procedure described in the text. Sugars induce a temperature shift of the denaturation curve more pronounced for trehalose, which increases with sugar content. The addition of sugar shifts and decreases the downshift of the amide I band (in lyso/D_2O/sugar mixtures) and thus decreases the solvent penetration inside the tertiary structure.

It is worth noting that the denaturation of lysozyme is shifted toward higher temperatures when it is dissolved in D_2O whether in the presence of sugars or not. In hydrated lysozyme, it was explained as stabilization of the native tertiary structure by the H-bond network of water which is stable on a wider temperature range in D_2O than in H_2O. However, Table 2 reveals that the energy of trehalose stabilization is slightly weaker in D_2O than in H_2O. This indicates that water−sugar interactions are crucial in the sugar bioprotective mechanism.

Discussion

This study reports converging experimental data on sugar bioprotective properties obtained from Raman scattering and MDSC investigations. It clearly shows occurrence of disaccharide-induced thermostabilization of the lysozyme structure at high temperatures and more particularly the most bioprotective effectiveness of trehalose to preserve folding helical molecular conformation upon heating. Figure 8 brings out the necessary use of complementary MDSC and Raman scattering experiments to carefully analyze the heat denaturation process and the

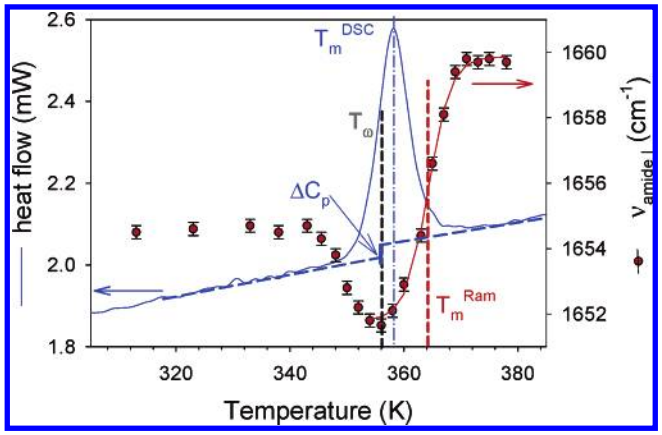

Figure 8. Representation of the two stages of the thermal denaturation from the temperature dependence of the amide I band frequency of the LW_dT40 sample. The plot of the heat flow trace reveals that the endothermic peak corresponds to the overlap of the two stages. The black and blue dashed vertical lines localized, respectively, T_ω and T_m reported in Table 1 and were determined from MDSC experiments. The red dotted line indicates the midpoint of the unfolding transition determined by the fitting procedure and the amide band frequency.

TABLE 2: Thermodynamical Parameters of the Unfolding Process in Lysozyme Obtained from the Analysis of the Amide I Band

samples	T_O^{Ram} (K)	T_m^{Ram} (K)	ΔT (K)	$\Delta(\Delta G_{ND})$ (kcal/ mol)
LW_h	346 ± 0.4	351.6 ± 0.3	2.2 ± 0.2	
LWhM40	349 ± 0.4	354.5 ± 0.3	2.7 ± 0.2	~1
LW_hS40	350 ± 0.4	355.8 ± 0.3	2.6 ± 0.2	~1
LW_hT40	354 ± 0.4	361.0 ± 0.3	3.1 ± 0.2	~2.3
LW_d	350 ± 0.4	354.1 ± 0.3	2.3 ± 0.2	
LW_dT20	354 ± 0.4	360.1 ± 0.3	2.6 ± 0.2	~0.5
LW_dT40	359 ± 0.4	364.3 ± 0.3	2.5 ± 0.2	~1.8

influence of sugars on the two stages of denaturation. The use of D_2O as a marker of water−protein interactions gives a direct description of these two stages. First, the transformation between the native tertiary structure and a transient more flexible structure with intact secondary structure is observed to be inherent to solvent penetration through the detection of enhanced isotopic exchange. Second, the unfolding of the secondary structure appears as a consequence of solvent penetration.

The first stage of denaturation was characterized by T_ω and ΔC_p, the temperature of transformation of the native tertiary structure determined from the peak of phase and the amplitude of the C_p jump associated with the first-order transition indicative and distinctive of a configurational entropy change upon denaturation. Both parameters are determined from MDSC experiments. Such changes and detailed kinetics of two-stage denaturation have been described in an earlier paper.[16]

Table 1 shows that addition of sugar leads to the increase of T_ω. This can be explained by considering that sugars distort the H-bond network of water. It can be observed (Figure 6b) that the distorted H-bond network of water is characterized by stronger O−H interactions in the presence of sugars. The main consequences are the stabilization of the native tertiary structure on an extended temperature range by increased solvent−protein interactions and a possible reduction of hydrophobic surface in contact with solvent in the protein interior. The frequency temperature dependence of the O−H stretching band (Figure 6b) in ternary mixtures reveals that intermolecular O−H interactions in water are stronger in the presence of sugar especially in the LW_hT40 mixture. Consequently, trehalose leads to the most increased extension of the stability domain of the native tertiary structure. This is confirmed by the observation of the frequency shift of the lowest-frequency band (Figure 6a) at a higher temperature in the LW_hT40 sample than in the other mixtures. Both the frequency shift of the lowest-frequency band and T_ω have been determined as signatures of the native state−molten globule state transition. This transformation is accompanied by an enhanced solvent accessibility probably responsible for a configurational entropy change which can be characterized by the measure of the C_p jump.

Table 1 brings out clearly that ΔC_p is not significantly influenced by the presence of sugar. This indicates that the increase of flexibility of the transient tertiary structure in the first stage of thermal denaturation is not dependent on the sugar content. However, it is clearly observed in Figure 1a that the C_p values, and probably the flexibility of proteins, are significantly lower in the presence of sugars. The lower flexibility of proteins in the presence of sugars, both in the native and in the transient tertiary structures, can be responsible for stabilizing the native tertiary structure and for stabilizing the secondary structure in the transient tertiary structure. Consequently, sugars contribute to preserve the very subtle equilibrium between hydrophobic and hydrophilic interactions responsible for the stability of the folding helical conformation, since most of the nonpolar groups are buried out of contact with water in the interior of the protein in its native state. This consideration can be confirmed by the limitation in the enhancement of the VDOS in the presence of sugars (Figure 3 and parts b, c, and d of Figure 4) previously observed accompanying the solvent penetration inside the protein[15] and also by the limitation in the downshift of the amide I band frequency prior to the unfolding process of the secondary structure in LW_dT samples. In this context, it can be assumed that the C_p jump is directly connected to the structural arrangement of the solvent after penetration inside the protein, rather than the quantity of penetrating solvent.

The latter consideration may also explain the influence of sugars on the second stage of denaturation, that is, the unfolding process of the secondary structure. Table 2 indicates that sugars contribute to the spread out unfolding of the secondary structure over a larger temperature range since ΔT increases with the addition of sugar. A lower exposure of hydrophobic surface to the solvent can also be considered as responsible for the extension of the unfolding process.

The study also shows a very weak difference between T_ω values in the ternary mixtures (Table 1) and a more pronounced difference between T_m values determined from the analysis of the amide I band frequency (Table 2). This difference observed between T_m^{Ram} values results merely from the two additional effects, that is, the increase of T_ω (Table 1) and ΔT (reported in Table 2 and corresponding to the temperature range of the unfolding process). Consequently, there is a very noticeable difference in the influence of the three sugars on the two stages of denaturation that lead cumulatively to a significant effectiveness of trehalose for the stabilization of the folding secondary structure of lysozyme.

It is well accepted that trehalose has privileged interactions with water that are considered responsible for the strong distortion of the H-bond network of water.[11−14] This property is probably at the origin of the strongest intermolecular O−H interactions in the H-bond network of water leading to the stabilization of the native tertiary structure.

The present study carried out on ternary mixtures with high water content undeniably demonstrates that the specific influence of trehalose on the structure of the H-bond network of water is at the origin of the exceptional capabilities of lysozyme to

preserve biological functions upon heating. Moreover, the different values of the energy trehalose stabilization ($\Delta[\Delta G_{ND}]$) obtained from the analysis of the unfolding process in LW_h-T40 and LW_dT40 samples indicate that the characteristics of water/sugar mixtures are involved to a great extent in the sugar-induced thermostabilization mechanism.

In a previous study,[40] the effectiveness of trehalose in the stabilization of proteins was determined as resulting from surface tension effect. In the present study, Raman investigations make it possible to probe simultaneously the H-bond network of water and the amide I band which is directly related to the fraction unfolded. The Raman scattering analysis brings out a precise description of the influence of sugars on the stability of the H-bond network of water (through the analysis of intermolecular O−H interactions) which is considered responsible for the stability of the native tertiary state. The analysis of three sugars with the same chemical formula and the same number of hydroxide groups allows us to assign the properties of trehalose in protein stabilization to topologic properties. The molecular conformation of trehalose is probably responsible for the modifications of the H-bond network of water which improve protein stability.

It is worth noting that the distortion of the tetrahedrally H-bonded network of water by trehalose is generally well adapted for the interpretation of the cryoprotective properties of trehalose.[7] This work shows that a consequence of the strengthening of intermolecular O−H interactions in the H-bond network of water contributes to the stabilization of the native tertiary structure and therefore inevitably to the stabilization of the folded state of the protein. The structure of the H-bond network of water is probably connected to the degree of flexibility of the protein. From the C_p analysis seen in Figure 1a, it can be expected that the addition of sugars induces a decrease in flexibility. It should be interesting to analyze the flexibility of lysozyme in the presence of different sugars and also to analyze simultaneously the influence of physical properties (molecular mobility) of the solvent and the solvent−lysozyme mixtures, on both the flexibility and the stability of the protein, as done at low temperatures.[30,36] It can be expected that the molecular mobility of water−sugar solutions are strongly coupled to the H-bond network of water and thus to the flexibility of the tertiary structure.

Acknowledgment. This work was supported by INTERREG III (FEDER) program and region Nord Pas-de-Calais. The authors are indebted to Professor G. P. Johari for stimulating and very helpful discussions.

References and Notes

(1) Allison, S.; Chang, B.; Randolph, T.; Carpenter, J. F. *Arch. Biochem. Biophys.* **1999**, *365*, 289.
(2) Sola-Penna, M.; Meyer-Fernandez, J.-R. *Arch. Biochem. Biophys.* **1998**, *360*, 10.
(3) Kreilgaard, L.; Frokjaer, S.; Flink, J.; Randolph, T.; Carpenter, J. F. *Arch. Biochem. Biophys.* **1998**, *360*, 121.
(4) Xie, G.; Timasheff, S. N. *Biophys. Chem.* **1997**, *64*, 25.
(5) Crowe, J. H.; Leslie, S. B.; Crowe, L. M. *Cryobiology* **1994**, *31*, 355.
(6) Green, J. L.; Angell, C. A. *J. Phys. Chem.* **1989**, *93*, 2880.
(7) Branca, C.; Magazu, S.; Maisano, G.; Migliardo, P. *J. Chem. Phys.* **1999**, *111*, 281.
(8) Branca, C.; Magazu, S.; Maisano, G.; Migliardo, F. *Phys. Rev. B* **2001**, *64*, 4204.
(9) Branca, C.; Magazu, S.; Maisano, G.; Migliardo, P.; Villari, V.; Sokolov, A. P. *J. Phys: Condens. Matter* **1999**, *11*, 3823.
(10) Magazu, S.; Maisano, G.; Migliardo, F.; Mondelli, C. *Biophys. J.* **2004**, *86*, 3241.
(11) Branca, C.; Magazu, S.; Migliardo, F.; Migliardo, P. *Physica A* **2002**, *304*, 314.
(12) Branca, C.; Maccarrone, S.; Magazu, S.; Maisano, G.; Bennington, S. M.; Taylor, J. *J. Chem. Phys.* **2005**, *122*, 174513.
(13) Lerbret, A.; Bordat, P.; Affouard, F.; Guinet, Y.; Hedoux, A.; Paccou, L.; Prevost, D.; Descamps, M. *Carbohydr. Res.* **2005**, *340*, 881.
(14) Lerbret, A.; Bordat, P.; Affouard, F.; Descamps, M.; Migliardo, F. *J. Phys. Chem. B* **2005**, *109*, 11046.
(15) Hédoux, A.; Ionov, R.; Willart, J. F.; Lerbret, A.; Affouard, F.; Guinet, Y.; Descamps, M.; Prevost, D.; Paccou, L.; Danède, F. *J. Chem. Phys.* **2006**, *124*, 14703.
(16) Salvetti, G.; Tombari, E.; Mikheeva, L.; Johari, G. P. *J. Phys. Chem. B* **2002**, *106*, 6081.
(17) Masaki, K.; Masuda, R.; Takase, K.; Kawano, K.; Nitta, K. *Protein Eng.* **2000**, *13*, 1.
(18) Azuaga, A. I.; Dobson, C. M.; Mateo, P. L.; Concejero-Lara, F. *Eur. J. Biochem.* **2002**, *269*, 4121.
(19) Privalov, P. L.; Potekhin, S. A. *Methods Enzymol.* **1986**, *131*, 4.
(20) Privalov, P. L. *J. Mol. Biol.* **1996**, *258*, 707.
(21) Lala, A. K.; Kaul, P. *J. Biol. Chem.* **1992**, *267*, 19914.
(22) Kuwajima, K. *Proteins* **1989**, *6*, 87.
(23) Kuwajima, K. *FASEB J.* **1996**, *10*, 102.
(24) Baum, J.; Dobson, C. M.; Evans, P. A.; Hanley, C. *Biochemistry* **1989**, *28*, 7.
(25) Militello, V.; Casarino, C.; Emanuele, A.; Giostra, A.; Pullara, F.; Leone, M. *Biophys. Chem.* **2004**, *107*, 175.
(26) Surewicz, W. K.; Mantsch, H. H.; Chapman, D. *Biochemistry* **1993**, *32*, 389.
(27) van-Stokkum, I. H.; Linsdell, H.; Hadden, J. M.; Haris, P. I.; Chapman, D.; Bloemendal, M. *Biochemistry* **1995**, *34*, 10508.
(28) Bustin, O.; Descamps, M. *J. Chem. Phys.* **1999**, *110*, 10982.
(29) Willart, J. F.; Descamps, M.; van Miltenburg, J. C. *J. Chem. Phys.* **2000**, *112*, 10992.
(30) Caliskan, G.; Kisliuk, A.; Tsai, A. M.; Soles, C. L.; Sokolov, A. P. *J. Chem. Phys.* **2003**, *118*, 4230.
(31) Novikov, V. N.; Duval, E.; Kisliuk, A.; Sokolov, A. P. *J. Chem. Phys.* **1995**, *102*, 4691.
(32) Saviot, L.; Duval, E.; Surovtsev, N.; Jal, J. F.; Dianoux, A. J. *Phys. Rev. B: Condens. Matter Mater. Phys.* **1999**, *60*, 18.
(33) Hedoux, A.; Derollez, P.; Guinet, Y.; Dianoux, A. J.; Descamps, M. *Phys. Rev. B: Condens. Matter Mater. Phys.* **2001**, *63*, 144202/1.
(34) Paciaroni, A.; Bizzarri, A. R.; Cannistraro, S. *Phys. Rev. E* **1999**, *60*, R2476.
(35) Diehl, M.; Doster, W.; Petry, W.; Schober, H. *Biophys. J.* **1997**, *73*, 2726.
(36) Caliskan, G.; Mechtani, D.; Roh, J. H.; Kisliuk, A.; Sokolov, A. P.; Azzam, S.; Cicerone, M. T.; Lin Gibson, S.; Peral, I. *J. Chem. Phys.* **2004**, *121*, 1978.
(37) Leslie, S. B.; Israeli, E.; Lightart, B.; Crowe, J. H.; Crowe, L. M. *Appl. Environ. Microbiol. J.* **1995**, *61*, 3592.
(38) Privalov, P. L. *Crit. Rev. Biochem. Mol. Biol.* **1990**, *25*, 281.
(39) Kunugi, S.; Tanaka, N. *Biochim. Biophys. Acta* **2002**, *1595*, 329.
(40) Kaushik, J. K.; Bhat, R. *J. Biol. Chem.* **2003**, *278*, 26458.